

## BRIEF COMMUNICATION

---

### SARCOMERE DISTRIBUTION PATTERNS IN SINGLE CARDIAC CELLS

NORA M. DE CLERCK, VICTOR A. CLAES, ERIK R. VAN OCKEN, AND DIRK  
L. BRUTSAERT *University of Antwerp, 2020 Antwerp, Belgium*

**ABSTRACT** Sarcomeres of single cardiac cells isolated either by microdissection or by enzymatic dissociation were visualized on a television screen, through the objective ( $63\times$ ) of an inverted microscope and a television camera. A distinct line of the television picture was positioned on the preparation and the frequency content, corresponding to the dark and light areas of the striations was tracked by a phase-locked loop. This technique permitted the measurement of the length of successive sarcomeres and hence the sarcomere distribution pattern over the entire preparation.

#### INTRODUCTION

Myocardial muscle mechanics have been closely related to changes in sarcomere length and sarcomere behavior, both in multicellular preparations (1–3) and in single cardiac cells (4). Determinations of sarcomere length in living mammalian cardiac muscle, either by photomicroscopy (3) or by laser diffraction (1), have been related to average values of sarcomere length without considering the distribution or the dynamics of the individual sarcomeres. Many questions remain as to the exact correlation between mechanical parameters and sarcomere behaviour, especially as to the effect of changing muscle length on individual sarcomere length and on their distribution along a well-determined segment length of the myofibrils.

#### METHODS

A new technique was developed that permits the measurement of sarcomere length along the length of a single cardiac cell. The analysis of the sarcomere distribution patterns can be combined with a detailed study of the mechanical behaviour of the entire preparation.

Single cardiac cells of the rat were isolated either by microdissection (5) or by enzymatic digestion (6) and were chemically skinned by detergent (Brij-58, polyethylene-20-cetyl-ether, Sigma Chemical Company, St. Louis, Mo.). One end of the cell was pinned down by a small bended hook fixed on a micromanipulator (De Fonbrune, Beaudouin, Paris). The remaining free end of the cell was attached to a movable needle, glued to a capacitance transducer, allowing simultaneous measurement of force, shortening, and velocity of shortening (7). All needles and hooks, used for fixing the cells, were made of glass and were pulled in a microforge (De Fonbrune). Contractions were initiated by calcium pulses induced by iontophoresis (5). All recordings of force, length, and velocity of shortening, together with

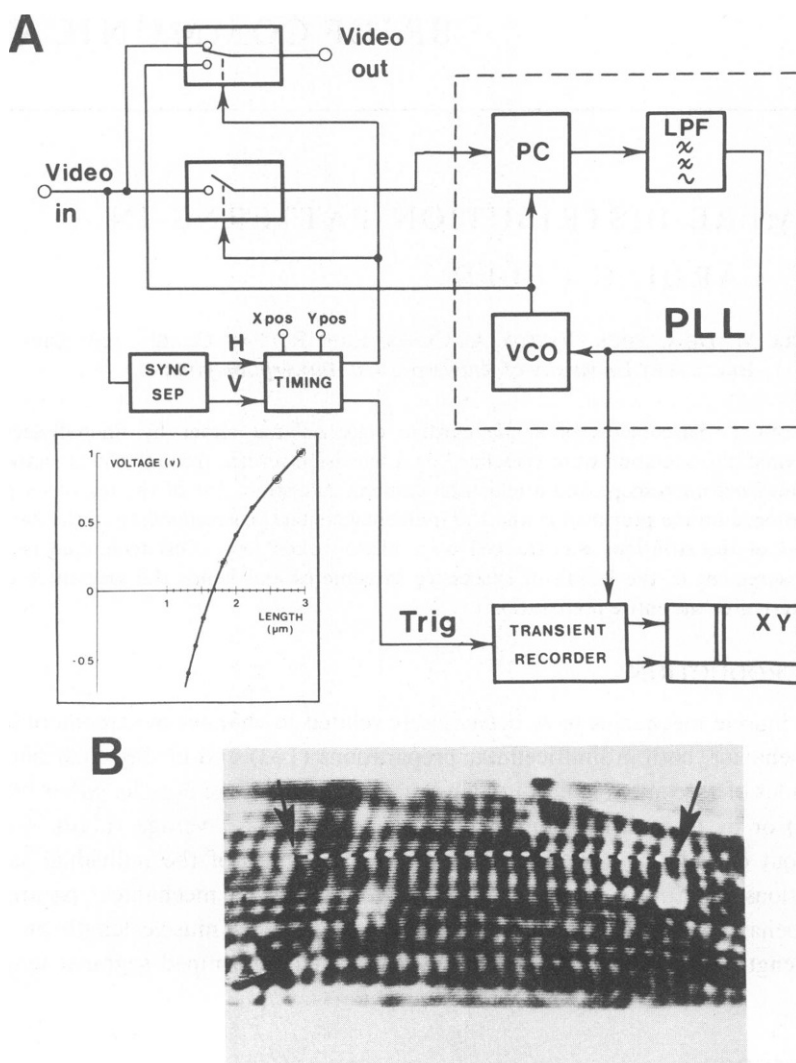


**FIGURE 1** *A*, block diagram of video and PLL circuits. Within dotted squares, PLL with PC, LPF, and VCO. Sync Sep; sync-pulse separator; with outputs H, horizontal sync pulse, and V, vertical sync pulse. The transient recorder is triggered by the timing circuit and buffers the data in its memory. These stored data are read out at a low speed and plotted on the XY-plotter. The insert shows the nonlinear relationship between output voltage and measured length. *B* shows a particular line (consisting of black and white spots) from the television image, while tracking the sarcomere pattern of a cell. The length of the measuring line was  $\sim 31 \mu\text{m}$ . Note that the black and white spots do not necessarily coincide with the striations, as long as the PLL is locked to the same frequency. An average sarcomere length of  $2.30 \mu\text{m}$  was measured in this cell, which was attached at both ends by two small glass hooks mounted on micromanipulators.

the activating calcium pulses, were displayed on a storage oscilloscope (Tektronix 611 Tektronix Inc., Beaverton, Ore.) and copied by means of a Hard Copy Unit (Tektronix 4601).

Sarcomeres were visualized on a television screen through an inverted microscope (Reichert—Biovert, Vienna) and a television camera (Sofretec CF 123N, Paris). The objective of the microscope (63 $\times$ ) projected the image of the cell and the sarcomeres on the target of a television camera tube. The camera could be rotated around its optical axis to align the longitudinal distribution of the sarcomere pattern in parallel with the television lines. An area of the cell was chosen in which the sarcomeres could be optimally visualized; in the course of each television frame, part of a distinct line of the television picture was selected and positioned on this particular part of the cell. During this measuring interval, a video gate was opened. Start and stop of the sample coincided with the beginning and the end of the sarcomere pattern of interest. Inasmuch as the scanning speed of the television system was constant, the frequency information contained in the video signal, corresponding to the area of the striations, could be related to the distance between successive light and dark transitions and hence to the length of the sarcomeres. This frequency content was tracked by a phase-locked loop (PLL), consisting of a voltage controlled oscillator (VCO), a phase comparator (PC), and a low-pass filter (LPF). These elements were connected in a feedback loop, forcing the VCO to track the frequency of the selected video portion (Fig. 1 A). The input voltage of the VCO represented a measure for the difference between the free-run frequency of the VCO and its input frequency. This "error voltage" was linearly proportional to the frequency of the appearance of the black and white striations of the sarcomeres. However, the distance between the successive sarcomeres, or the sarcomere length, corresponded to the period of the video signal. Therefore, the sarcomere length was related to the measured voltage in a nonlinear, but hyperbolic way, as depicted by the insert in Fig. 1 A.

The PLL system could follow shifts in frequency of the video signal and therefore variations in the distribution of the length of successive sarcomeres. To check the accuracy of the tracking of the sarcomere pattern by the PLL, the output of the VCO (a square wave) was mixed with the video signal during the sample interval only, resulting in a line of black and white dots superimposed on the image of the preparation. When the black and white dots did not move and were aligned with the sarcomere pattern, the PLL was tracking properly and valid measurements were obtained. The position and the length of this line could be selected and determined the sampled portion of the picture and the sampling duration. Each distribution sample could be acquired in  $<60\ \mu\text{s}$  with a sampling rate of  $50\ \text{s}^{-1}$ . The output of the PLL was connected to an oscilloscope and to a transient recorder (Biomation 802, Palo Alto, Calif.). This latter information was then plotted on an XY-recorder (Hewlett-Packard 7004B Hewlett-Packard Co., Palo Alto, Calif.). The output voltage vs. frequency characteristic of the PLL was calibrated electronically with a frequency counter and a sine wave oscillator; a horizontal reference line of  $1.66\ \mu\text{m}$  was determined by tracking the image of a diffraction grating of 600 lines/mm. The overall accuracy of the system was of the order of 1%.

## RESULTS

Fig. 1 B illustrates the tracking system: a distinct line consisting of black and white dots is shown tracking the sarcomere pattern of a cell attached at both ends by two bended hooks mounted on two separate micromanipulators. Fig. 2 A depicts a sarcomere distribution pattern (area between arrows); the tiny lines were drawn on the pattern to illustrate the digitizing procedure: every  $0.5\ \mu\text{s}$ , all samples of the pattern were digitized, and using a computer program, average sarcomere length could be calculated; in this case it was  $2.37 \pm 0.01\ \mu\text{m}$  (Mean  $\pm$  SE of 17 samples). Fig. 2 B shows two superimposed sweeps of the slack sarcomere distribution over part of a cell that was lying unattached at the bottom of the perfusion chamber. Note the relative uniformity among subsequent sarcomere lengths in the measured segment. Similarly, in 12 cells of the rat, slack length was determined in different regions, yielding an average value of  $1.85 \pm 0.02\ \mu\text{m}$  (Mean  $\pm$  SE).

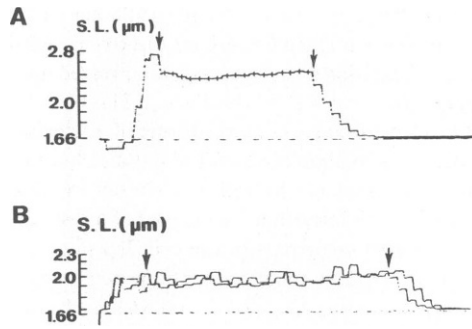


FIGURE 2 *A* illustrates a sarcomere distribution pattern (area between arrows). The scale on the ordinate indicates reference values for sarcomere length;  $1.66\ \mu\text{m}$  corresponds to the calibration. The scale is only meant as an estimate: a computer program was used for all calculations. The vertical ticks were drawn on the sarcomere distribution pattern to illustrate the digitizing procedure, used for calculating the average sarcomere length, in this case  $2.37 \pm 0.01\ \mu\text{m}$  (mean  $\pm$  SE of 17 samples). *B* depicts a typical sarcomere distribution pattern of a nonattached free cell at slack length. Routinely, two sweeps were recorded to check that the same sarcomere region was analyzed. The scale on the ordinate indicates reference values for sarcomere length;  $1.66\ \mu\text{m}$  corresponds to the calibration. The arrows indicate the area ( $33\ \mu\text{m}$  long) of the cell in which sarcomere length is measured. The pattern outside the area delineated by the arrows are start and stop artefacts due to the acquisition time ( $2\ \mu\text{s}$ ) of the PLL. Average sarcomere length in this cell was  $1.96 \pm 0.01\ \mu\text{m}$  (Mean  $\pm$  SE,  $n = 53$ ).

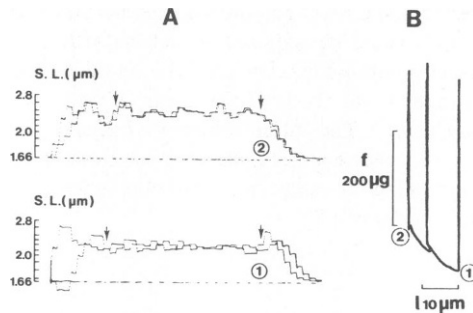


FIGURE 3 *A* shows two sarcomere patterns at two different preloads and thus at two different initial cell lengths. Average sarcomere length in pattern 1 was  $2.18 \pm 0.01\ \mu\text{m}$  (Mean  $\pm$  SE,  $n = 48$ , measured over  $\sim 30\ \mu\text{m}$ ); in pattern 2,  $2.41 \pm 0.01\ \mu\text{m}$  (Mean  $\pm$  SE,  $n = 44$ , over  $28\ \mu\text{m}$ ). Similar experiments were performed over a range of sarcomere lengths varying from  $1.7$  to  $\sim 2.5\ \mu\text{m}$ . Longer sarcomere lengths were more difficult to impose as the movable needle detached too easily. During the experiments, at room temperature, the cells were constantly perfused with a solution containing (mM) NaCl 132,  $\text{MgCl}_2 \cdot 6\text{H}_2\text{O}$  4,  $\text{Na}_2\text{ATP}$  5, glucose 7, imidazole 18, EGTA 0.125. Before the actual experiments, cells were treated with a skinning solution containing a total EGTA concentration of  $0.5\ \text{mM}$ , and a total of  $0.5\%$  Brij-58, in order to destroy all membranous systems (10). In this study a total number of 36 suitable cells were analyzed, 27 of which were isolated by microdissection. These cells had an average length of  $89 \pm 4\ \mu\text{m}$  (Mean  $\pm$  SE,  $n = 36$ ) and an average width of  $20 \pm 1\ \mu\text{m}$  (Mean  $\pm$  SE,  $n = 36$ ). *B* shows the mechanical behaviour of the cell;  $f$  (force) vs.  $l$  (length). At different cell lengths, contractions were initiated by the iontophoretic release of known amounts of calcium ions. Isometric contractions were recorded. A maximum active force of  $411\ \mu\text{g}$  was reached at an average sarcomere length of  $2.18\ \mu\text{m}$  with submaximal activation.

In the experiment shown in Fig. 3, the cell was first fixed at one end by a small glass hook directed by a micromanipulator. The other end was then attached to the movable needle mounted on the force transducer system. The initial length of the cell was changed by increasing the preload imposed on the cell by the transducer system. Note in Fig. 3 *A* the increase in average sarcomere length from 2.18  $\mu\text{m}$  in pattern 1 to 2.41  $\mu\text{m}$  in pattern 2. Hence, increasing the initial length of the cell by enhancing the preload resulted in lengthening of the underlying sarcomeres. In 15 representative experiments a ratio between the change in initial length of the cell, and the change in average sarcomere length of  $0.74 \pm 0.04 \mu\text{m}$  (Mean  $\pm$  SE) was observed. In Fig. 3 *B*, isometric contractions were initiated by iontophoretically released calcium ions. Although, in accordance with the familiar length-active force relation of muscle, maximal force development was obtained at a well-determined preload and the curves relating active force development to either initial cell length or sarcomere length were not very steep.

Fig. 4 shows an experiment under isotonic conditions at two different cell lengths: here the preload was changed while keeping total load during shortening at a constant level. In Fig. 4 *A* the sarcomere distribution patterns are shown at the two different initial cell lengths. In pattern 1 average sarcomere length was 1.80  $\mu\text{m}$ , and in pattern 2 it was 1.96  $\mu\text{m}$ . At these two lengths, an afterloaded isotonic contraction was initiated by a calcium pulse. Despite the marked change in initial sarcomere length, the cell shortened to the same extent; this shortening occurred with the same velocity of shortening at all lengths during shortening, regardless of the time at which this length was attained. This unique relationship between

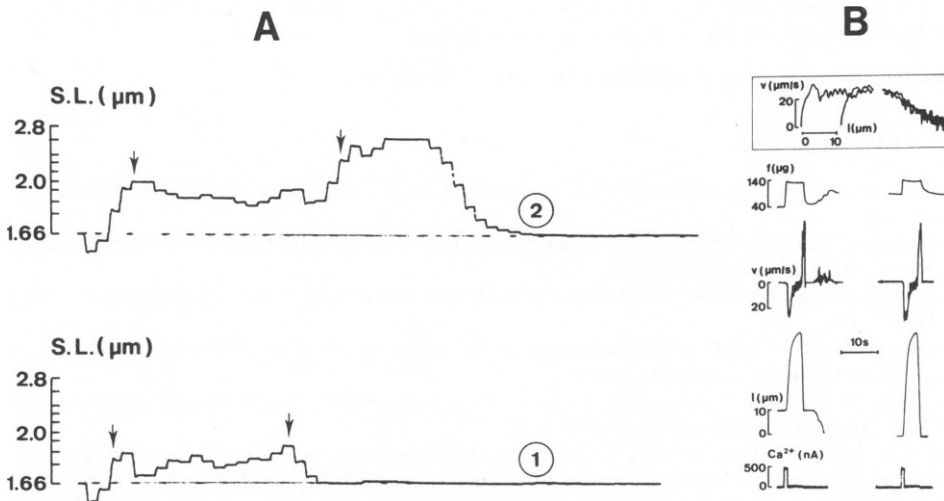


FIGURE 4 *A* shows two sarcomere patterns at two different preloads and thus at two different initial lengths of the cell. Average sarcomere length in pattern 1 was  $1.80 \pm 0.01 \mu\text{m}$  (Mean  $\pm$  SE,  $n = 16$ , length of measurement  $\sim 20 \mu\text{m}$ ) and in pattern 2,  $1.96 \pm 0.01 \mu\text{m}$  (Mean  $\pm$  SE,  $n = 18$ , length of measurement  $\sim 23 \mu\text{m}$ ). *B*, isotonic afterloaded contractions induced by the same amount of calcium ions are shown as a function of time, at the same total load ( $f$ ). Notice that at the same  $f$ , despite the change in average sarcomere length, the cell shortens ( $l$ ) to the same extent and reaches the same peak velocity of shortening ( $v$ ). The upper panel shows the phase plane  $v$  as a function of instantaneous length ( $l$ ). Notice that except for the initial portion due to the different starting lengths, these  $v$ - $l$  traces perfectly coincide during shortening.

velocity of shortening and length during shortening, regardless of the starting length and time during shortening, was demonstrated by simultaneously displaying phase-plane velocity-length traces of the same two contractions. Except for the initial portion, which was due to the different starting lengths, these velocity-length traces perfectly coincided during shortening. These results indicated that in a single cell, activated by a given amount of calcium ions within the studied range of sarcomere lengths, changing the initial length of the sarcomeres does not induce alterations in the extent of shortening nor in velocity of shortening at any length during shortening. These results are in line with previous observations in intact cardiac muscle (8, 9), and again reconfirm the fundamental nature of this relationship.

## DISCUSSION

This new technique permitted not only the measurement of average sarcomere length, but also the analysis of the distribution patterns of the different sarcomere lengths in different regions of the preparations. The results indicated that changes in mechanical parameters measured at the level of a single cell, do indeed reflect changes in sarcomere length. In particular, altering the initial length of the cell affected average sarcomere length, despite minor differences in the distribution of the lengths of the individual sarcomeres in series as shown by the sarcomere patterns. The deviation from 1 of the ratio between a change in sarcomere length and a change in cell length is most likely due to some series elasticity at the points of attachment. The possibility of combining the detailed mechanical analysis of a single cell (simultaneous recording of force, shortening, and velocity of shortening) with the distribution of individual sarcomere lengths, opens wide perspectives for the further study of the contractile behaviour of the sarcomere as a basic unit of cardiac contraction.

*Received for publication 2 June 1980 and in revised form 17 March 1981.*

## REFERENCES

1. Pollack, G. H., and J. W. Krueger. 1976. Sarcomere dynamics in intact cardiac muscle. *Eur. J. Cardiol.* 4:53-65.
2. Pollack, G. H., and L. L. Huntsman. 1974. Sarcomere length-active force relations in living mammalian cardiac muscle. *Am. J. Physiol.* 277:383-389.
3. Julian, F. J., and M. R. Sollins. 1975. Sarcomere length-tension relations in living rat papillary muscle. *Circ. Res.* 37:299-383.
4. Fabiato, A., and F. Fabiato. 1975. Dependence of the contractile activation of skinned cardiac cells on the sarcomere length. *Nature (Lond.)* 256:54-56.
5. De Clerck, N. M., V. A. Claes, and D. L. Brutsaert. 1977. Force-velocity relations of single cardiac muscle cells: calcium dependence. *J. Gen. Physiol.* 69:221-241.
6. Powel, T., and V. W. Twist. 1976. A rapid technique for the isolation and purification of adult cardiac muscle cells having respiratory control and a tolerance to calcium. *Biochim. Biophys. Res. Commun.* 72:327-333.
7. Brutsaert, D. L., V. A. Claes, and N. M. De Clerck. 1978. Relaxation of mammalian single cardiac cells after pretreatment with the detergent Brij-58. *J. Physiol. (Lond.)* 283:481-491.
8. Brutsaert, D. L., and E. H. Sonnenblick. 1969. Force-velocity-length-time relations of the contractile elements in heart muscle of the cat. *Circ. Res.* 24:137-149.
9. Brutsaert, D. L. 1974. The force-velocity-length-time interrelation of cardiac muscle. In *The Physiological Basis of Starling's Law of the Heart*. Ciba Foundation Symposium 24 (new series). Elsevier/North-Holland Biomedical, Amsterdam. 155-157.
10. Orentlicher, M., J. P. Reuben, H. Grundfest, and P. W. Brandt. 1974. Calcium binding and tension development in detergent-treatment muscle fibres. *J. Gen. Physiol.* 63:168-186.